บทความวิชาการ

ปรากฏการณ์จลนศาสตร์เชิงอิเล็กตรอนและการจัดการการไหลภายในท่อระดับไมโครเมตร

ปนัดดา เดชาดิลก*

บทคัดย่อ

ปรากฏการณ์จลนศาสตร์เชิงอิเล็กตรอนในท่อระดับไมโครเมตรได้รับความสนใจเนื่องจากถูกประยุกต์ใช้ในการสร้างการไหลและการควบคุมความเร็วของไหลในระบบของไหลจุลภาค (microfluidic systems) บทความนี้ทบทวนและอภิปรายการไหลแบบตัวเลขเรย์โนลด์ต่ำระหว่างการเกิดอิเล็กโตรออสโมซิส กระแสสตรีมมิง และศักย์สตรีมมิง เมื่อท่อระดับไมโครเมตรบรรจุสารละลายอิเล็กโตรไลต์ กลุ่มเคาน์เตอร์ไอออนจะก่อตัวขึ้น ณ บริเวณรอยต่อระหว่างของแข็งและของไหลซึ่งมีประจุไฟฟ้า กลุ่มเคาน์เตอร์ไอออนนั้นถูกเรียกว่าชั้นประจุไฟฟ้าคู่ (electrical double layer) การไหลแบบอิเล็กโตรออสโมติกเกิดจากการเคลื่อนที่ของเคาน์เตอร์ไอออนดังกล่าวเนื่องจากความต่างศักย์ภายในท่อ ขณะที่กระแสสตรีมมิง คือกระแสไฟฟ้าซึ่งเกิดขึ้นแม้เมื่อความต่างศักย์ระหว่างปลายท่อทั้งสองด้านมีค่าเท่ากับศูนย์เนื่องจากเคาน์เตอร์ไอออนในชั้นทวีคูณไฟฟ้าถูกพัดพาโดยการไหลที่เกิดจากความต่างของความดันภายในท่อ ส่วนศักย์สตรีมมิงคือความต่างศักย์ซึ่งเกิดขึ้นเมื่อมีความต่างของความดันที่ปลายท่อทั้งสองด้านเพราะกระแสไฟฟ้าภายในวงจรเปิด (open circuit) มีค่าเท่ากับศูนย์ การประยุกต์ใช้ในระบบของไหลจุลภาคของปรากฏการณ์จลนศาสตร์เชิงอิเล็กตรอนทั้งสามล้วนได้รับการอภิปราย

คำสำคัญ: ปรากฏการณ์จลนศาสตร์เชิงอิเล็กตรอน อิเล็กโตรออสโมซิส กระแสสตรีมมิง ศักย์สตรีมมิง ระบบของไหลจุลภาค

ภาควิชาฟิสิกส์ คณะวิทยาศาสตร์ จุฬาลงกรณ์มหาวิทยาลัย

*ผู้นิพนธ์ประสานงาน, e-mail: panadda.D@chula.ac.th

Electrokinetic Phenomena and Manipulation of Flows in Microchannels

Panadda Dechadilok*

ABSTRACT

Electrokinetic phenomena have gained attentions due to applications in generation of flow and manipulation of fluid velocity in microfluidic systems. The article presented here reviews and discusses low Reynolds fluid flows during the occurrences of electroosmosis, streaming current, and streaming potential, each with its unique feature. If an electrolytic solution is confined in a channel, a cloud of counter-ions, referred to as an electrical double layer, are formed near the charged solid-fluid interfaces. A velocity of an electroosmotic flow is generated by motion of counter-ions due to potential difference in the channel. Streaming current, an electric current observed despite the absence of potential difference, is generated by motion of counter-ions in the electrical double layer carried by a fluid flow caused by pressure difference across the channel. Streaming potential, a potential difference generated by a difference in pressure at channel ends, is due to the zero current condition of an open-circuit system. Microfluidic applications of the three electrokinetic phenomena are also discussed.

Keywords: Electrokinetic phenomena, electroosmosis, streaming current, streaming potential, microfluidics

Department of Physics, Faculty of Science, Chulalongkorn University

*Corresponding author, e-mail: panadda.D@chula.ac.th

Introduction

Microfluidics refers to devices and methods employed in manipulating fluid flow with length scale of 10-100 μm or smaller. Fabrication and utilization of microfluidic devices have gained a lot of interest due to applications in biotechnology such as high-resolution separations and detections that require very small volumes of samples (less than 1 μL) where a microchannel can be replicated into a network of many channels [1-3]. Microfluidic devices can also be employed as a tool to perform fundamental studies of chemical, physical and biological processes on a cellular length scale [4]. Electrokinetic phenomena, a coupling between electric currents and fluid flow of electrolytic solution, have received attentions as a way to control flow in microchannels. If the channel surfaces are charged and it contains an electrolytic solution, a diffuse region of small counterions, known as the electrical double layer, is formed near the charged interfaces [5, 6]. This article focuses on reviewing and discussing fluid mechanics of three different electrokinetic phenomena: electroosmosis, streaming potential and streaming current, under a condition that the thickness of the electrical double layer, often referred to as a Debye screening length, is comparable to the dimensions of the microchannels. First, the Nernst-Planck equation describing the ion fluxes and the Poisson-Boltzmann equation are introduced. Then, the calculation of an electric current and fluid volumetric flow rate as a function of pressure gradient and imposed electric field will be discussed, followed by the definitions of electroosmosis, streaming potential and streaming current. An analytical solution is obtained for channels with weakly charged surfaces and the different fluid flow profiles during the three electrokinetic phenomena would be compared. Finally, applications of electroosmosis, streaming potential and streaming current are reviewed.

Ion fluxes, electrical double layer and Debye screening length

According to the Nesrnst-Planck equation, the fluxes of small cations and anions in an ideal and dilute electrolytic solution can be written as follows.

$$\vec{N}_i = C_i\vec{v} - D_i\left[\vec{\nabla}C_i + z_iC_i\left(\frac{e}{kT}\right)\vec{\nabla}\psi\right] \tag{1}$$

where $\vec{N}_i$ and C_i are the flux and concentration of ion i, respectively, and z_i is its valence. D_i is the diffusivity of ion i. $\vec{v}$ is the fluid velocity. k is the Boltzmann's constant, whereas T is the absolute temperature, and e is the elementary charge [7]. The first term on the right hand side of Eq.(1) is the convective term, whereas the second and third terms are the diffusive term and the electromigration term, a movement of ions due to an electric field, respectively. ψ is the electrical potential, related to the volumetric charge density (ρ_e) by the Poisson's equation as shown below.

$$\nabla^2\psi = \frac{-\rho_e}{\varepsilon} = \frac{-e\sum_i z_i C_i}{\varepsilon} \tag{2}$$

where ε is the dielectric permittivity of the electrolytic solution. For a system in equilibrium where the fluid is stationary and the convective term of the ion fluxes is absent, the diffusive and electromigration terms of the Nearst-Planck equation are balanced, resulting in the ion concentration obeying a Boltzmann distribution:

$$C_i = C_{i\infty} \exp\left(-z_i e\psi/kT\right). \tag{3}$$

$C_{i\infty}$ is the ion concentration at the location where $\psi = 0$. Substituting the ionic concentration from Eq. (3) into Eq. (1) results in the Poisson equation becoming the Poisson-Boltzmann equation as shown below.

$$\nabla^2\psi = \frac{-e}{\varepsilon}\sum_i z_i C_{i\infty} \exp\left(-\frac{z_i e\psi}{kT}\right) \tag{4}$$

If the electrolytic solution contains univalent-univalent electrolytes ($z_+ = 1$ and $z_- = -1$) and the bulk external electrolytic solution (outside the channel) is electroneutral ($C_{+\infty} = C_{-\infty} = C_\infty$), Eq. (4) can be rewritten as

$$\nabla^2\phi = \frac{\sinh\phi}{\lambda^2} \tag{5}$$

where ϕ is the electric potential scaled with the thermal energy ($\phi = e\psi/kT$.), and λ is the Debye screening length defined as

$$\lambda = \left(\frac{2e^2 C_\infty}{\varepsilon kT}\right)^{-1/2} \tag{6}$$

From Eq. (5), it can be seen that the Debye screening length is the length scale of the system. As indicated in Eq. (6), λ varies as a function of $C_\infty^{-1/2}$, and the Debye screening length can be altered by adjusting C_∞. The higher C_∞ is, the smaller the Debye screening length becomes. As will be discussed further in the next section, the value of the Debye screening length strongly affects the flow profiles in charged microchannels.

Another observation from Eq. (5) is that the thermal potential (thermal energy divided by elementary charge or kT/e), is the scale for the electric potential. At 25°C, the thermal potential is approximately 25 mV. For a system where $|\psi| << kT/e$ ($|\phi| << 1$.), the hyperbolic sine term of Eq. (5) can be approximated as a Taylor expansion as follows.

$$\sinh\phi \approx \phi + O(\phi^2) \tag{7}$$

The approximation shown in Eq.(7) is referred to as the Debye-Huckel approximation where $O(\phi^2)$ represents the error of including only the first term in the Taylor expansion (Eq. (7). The error is on the order of ϕ^2. When the first term in the above Taylor expansion is substituted

back into Eq. (5), we obtain

$$\nabla^2\phi \approx \frac{\phi}{\lambda^2} \tag{8}$$

Equation (8) is referred to as the linearized Poisson-Boltzmann equation. As an example, a channel consisting of two charged parallel infinite plates is considered. As shown in Fig. 1, y is the distance from the mid-plane, whereas $y = 0$ is the location of the mid-plane of the channel with equal distances from both plates. The distance between the plates is $2H$ and the potential on the channel surfaces is assumed to be constant at ψ_0, leading to a following boundary condition;

$$\phi\left(y = \pm H\right) = \frac{\psi_0}{\left(kT/e\right)}. \tag{9}$$

A solution of the linearized Poisson-Boltzmann equation obtained analytically is written as

$$\phi = \frac{\phi_0}{\cosh\left(H/\lambda\right)} \cosh\left(\frac{y}{\lambda}\right) \tag{10}$$

where ϕ_0 is the dimensionless channel potential defined as $\phi_0 = \frac{e\psi_0}{kT}$. The scaled electrical potential profile is presented as a function of y in Fig. 2 for various values of Debye screening length (λ). Equation (10) indicates that the Debye screening length is truly the length scale for the electrical potential within the channel. As shown in Fig. 2, at locations where the distance from the channel walls is much larger than λ, ϕ vanishes. So does the volumetric charge density (ρ_e) that is proportional to its second derivative. The Debye screening length is, therefore, often viewed as the “thickness” of the electrical double layer because of the non-zero concentration of counter-ions located as shown schematically in Fig. 1. It is important to note that the sign of the counter-ions is always opposite to that of charges on the channel surface.

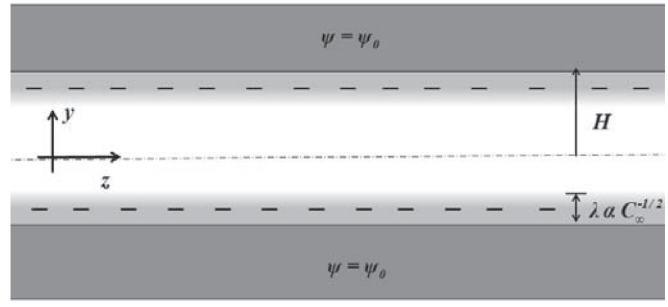

Figure 1. Schematic drawing of a cross-section of channel consisting of parallel infinite plates with identical surface potential ($\psi_0 > 0$). The mid-plane (at $y = 0$) is indicated by the dot-dashed line, where as the distance between the plates is $2H$. A stationary electrolytic solution is contained between the plates. Diffuse regions of counter-ions (cations), referred to as the electrical double layers, are formed near the liquid-solid interfaces. The Debye screening length, λ, is proportional to $C_\infty^{-1/2}$. Transverse locations with distances from the plates less than or equal to λ, the Debye screening length, are represented by "-" charges and shaded area.

It is worth noting that using the Debye-Huckel approximation in the calculation will likely to overestimate the value of ϕ. The solution of the nonlinear Poisson-Boltzmann equation (Eq.(5)) is always less than the analytical solution of the linearized Poisson-Boltzmann equation (Eq. (8)) with the discrepancy increasing as ϕ_0 increases.

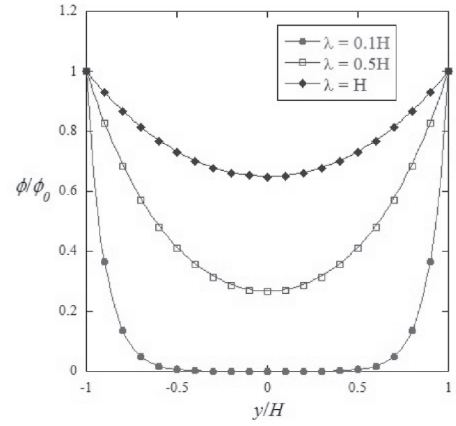

Figure 2. A solution of the linearized Poisson-Boltzmann equation : dimensionless surface potential ($\phi/\phi_0=\psi/\psi_0$) inside a channel consisting of two parallel plates with identical surface potential (Fig. 1). Results are plotted as a function of distance from the mid-plane (y) scaled with the channel half-width (H) for the cases where the Debye screening length equals the channel half-width (a line with diamonds), a quarter of the channel width (a line with squares), and one-twentieth of the channel width (a line with circles).

Electric current, fluid velocity and volumetric flow rate of electrolytic solutions in charged channels

Up until now, only the stationary electrolytic solution in a charged microchannel is considered. In this section, a calculation of fluid velocity and electrical potential in a channel containing the electrolytic solution that is moving due to two driving factors, a pressure gradient and an imposed electric field, will be discussed. The first parameter to be considered is the Reynolds number (Re) characterizing the flow defined as

$$\mathrm{Re} = \frac{L^2/(\eta/\rho)}{L/U} = \frac{\rho UL}{\eta} \tag{11}$$

where L and U are the length scale and velocity scale of the flow in the channel, respectively. ρ and η are the fluid density and shear viscosity. As shown in Eq.(11), the Reynolds number is the ratio between the estimated time scale of viscous dissipation $\left(\tau_{\text{viscous}} = \frac{L^2}{\eta/\rho}\right)$ and the estimated time scale of convection of momentum $\left(\tau_{\text{convection}} = \frac{L}{U}\right)$. The rule of thumb is that the "faster" process (with smaller time scale) controls the transport of momentum and mechanical energy within the flow. If Re >> 1, convection plays a prominent role in momentum transport, whereas the effect of viscous dissipation can be neglected (except at a region near solid surfaces referred to as a boundary layer). On the other hand, if Re << 1, viscous dissipation dominates.

High Reynolds number flows involve small kinematic viscosities, large velocities and large length scales. Flows observed in daily life (such as those of air and water) are generally characterized by high Re, and observed phenomena include separations of streamlines, formations of eddies, and if Re is above the critical Reynolds number, turbulence. Low Reynolds number flows, also referred to as creeping flows or Stokes flows, however, are seen in systems with small length scales, small velocities or large kinematic viscosities. These flows exhibit distinct properties that are very different from those of high Reynolds number flows seen in daily life. An example is flow reversibility. If a drop of color dye is gently placed in a Taylor-Couette system consisting of viscous fluid contained in a space between two concentric cylinders and the inner cylinder is rotated slowly in a counter-clockwise such that Re is very low, the color dye will mix with the fluid. However, if the cylinder is once again rotated but in a clockwise direction, the color dye will reverse back to being a drop (in an approximate sense) when the number of turns of the cylinder rotation in the clock wise direction equals the number of turns of the cylinder rotation in the counter-clockwise direction [8]. For a pseudo-steady creeping flow characterized by low Reynolds number, time enters only as a parameter, and the fluid velocity

and pressure respond almost instantaneously to changes in movement of surfaces [7]. Mixing and "unmixing" the fluid can be achieved by changing the direction of the mixer.

For various circumstances concerning flows in microchannels, the Reynolds number is small [4]. As an example, a channel with circular cross-section containing an electrolytic solution with the shear viscosity close to that of water (on the order of 10^{-3} Pa.s at room temperature) is considered. If the cross-section radius, R, is on the order of 1 μm, and the speed of the electrolytic solution is a typical fluid speed of 1 cm/s, Re is 0.01. In the work presented here, only systems with Re << 1 will be discussed.

In order to investigate the electrokinetic effect on fluid flow, the calculation of fluid velocity and electric current in a channel with constant surface density and circular cross-section will be presented as an example. The channel is assumed to be very long with its length much larger than its radii such that for most axial position, the entrance effect on flow profile is small. As a result, the electrolytic flow is unidirectional, fully-developed and steady. An electric field in the axial direction (E_z) is uniform. Because Re << 1, the Navier-Stokes equation becomes the Stokes equation with the electrical body force term as shown below.

$$\frac{dP}{dz} = \frac{\eta}{r}\frac{\partial}{\partial r}\left(r\frac{\partial v_z}{\partial r}\right) + E_z\rho_e \tag{12}$$

where v_z is the fluid velocity within the channel which is unidirectional. r and z are the radial and axial positions, respectively. P is the pressure, and the term on the left hand side of Eq. (12), dP/dz, is the pressure gradient in the axial direction. The first term on the right hand side of the equation is the effect of viscous dissipation on the force balance, whereas the second term is the electrical force per unit volume.

The governing equation for an electrical potential, the Poisson Equation (Eq.(2)), becomes

$$\frac{1}{r}\frac{\partial}{\partial r}\left(r\frac{\partial \psi}{\partial r}\right) = \frac{-\rho_e}{\varepsilon} \quad . \tag{13}$$

The absence of $\partial^2\psi/\partial z^2$ is due to the fact that the axial electric field, E_z, is constant. A relationship between v_z, E_z, ψ and dP/dZ can be obtained from substituting Eq.(13) into Eq.(12) and integrating twice under conditions that $v_z(r = R) = 0$ (a no-slip boundary condition at the channel surface), and that both v_z and ψ are finite at the channel centerline ($r = 0$). v_z is as a function of E_z and the axial pressure gradient as follows [9].

$$v_z = E_z\frac{\varepsilon}{\eta}\left[\psi(r,z) - \psi(0,z)\right] - \frac{1}{4\eta}\frac{dP}{dz}\left[R^2 - r^2\right] \tag{14}$$

where R is the radius of the channel cross-section. The fluid flow rate (Q), the total volume of fluid transported per unit time, is calculated as shown below.

$$Q = 2\pi\int_0^R v_z r dr = E_z \frac{2\pi\varepsilon}{\eta}\int_0^R r\left[\psi(r,z)-\psi(0,z)\right]dr - \frac{\pi R^4}{8\eta}\frac{dP}{dz}. \tag{15}$$

The second terms on the right hand side of Eqs. (14) and (15) are the fluid velocity and the flow rate of a Poiseuille flow in an uncharged channel with circular cross-section, respectively. The first terms on the right hand side of the equations, on the other hand, are the contribution of E_z to fluid motion.

Under an assumption that the electrical double layer maintains its equilibrium structure despite the imposed electric field, [$\psi(r, z)$-$\psi(0, z)$] does not depend on the axial position (z). The ion concentration does not vary in the z-direction, and the diffusion term in the Nernst-Planck equation is absent, causing the current density (i_z) to be written as

$$i_z = e\sum_i z_i N_{iz} = \kappa_e E_z + \rho_e v_z \tag{16}$$

where the fluid electric conductivity, κ_e, is

$$\kappa_e = \frac{e^2}{kT}\sum_i z_i^2 D_i C_i. \tag{17}$$

From the above expression of the current density, the total current, I, can be obtained as

$$I = 2\pi\left[E_z\int_0^R r\kappa_e dr + \int_0^R r v_z \rho_e dr\right]. \tag{18}$$

Substituting Eq.(16) into Eq.(18) yields

$$I = 2\pi\left[\begin{array}{l} E_z\left(\displaystyle\int_0^R r\kappa_e dr - \frac{\varepsilon^2}{\eta}\int_0^R\left(\psi(r,z)-\psi(r=0,z)\right)\frac{\partial}{\partial r}\left(r\frac{\partial\psi}{\partial r}\right)dr\right) \\ +\varepsilon\dfrac{dP}{dz}\displaystyle\int_0^R\frac{\left(R^2-r^2\right)}{4\eta}\frac{\partial}{\partial r}\left(r\frac{\partial\psi}{\partial r}\right)dr \end{array}\right]. \tag{19}$$

To obtain the explicit expressions for v_z, Q and I, it is necessary to evaluate the difference between the electric potential, ψ, and the potential on the centerline of the channel, $\psi(r = 0, z)$. Similarly to obtaining the solution of the Poisson-Boltzmann equation for a channel containing a stationary electrolytic solution discussed above, an analytical solutions for an electric potential and a fluid velocity inside a channel containing a driven electrolytic solution can be obtained by using a Debye-Huckel approximation as will be stated below.

Electroosmosis, streaming current and streaming potential

Equations (15) and (19) combined yield a relationship between the fluid flow rate, the electric current and the driving factors that cause fluid motion (the pressure gradient and the electric field) as follows.

$$\begin{bmatrix} Q \\ I \end{bmatrix} = \begin{bmatrix} M_{11} & M_{12} \\ M_{21} & M_{22} \end{bmatrix} \begin{bmatrix} -dP/dz \\ E_z \end{bmatrix} \tag{20}$$

where

$$M_{11} = \frac{\pi R^4}{8\eta}. \tag{21a}$$

$$M_{12} = M_{21} = \frac{-\pi\varepsilon}{\eta}\int_0^R r^2 \left(\frac{\partial \psi}{\partial r}\right) dr. \tag{21b}$$

$$M_{22} = 2\pi\left[\left(\int_0^R r\kappa_e dr - \frac{\varepsilon^2}{\eta}\int_0^R \left(\psi(r,z) - \psi(r=0,z)\right)\frac{\partial}{\partial r}\left(r\frac{\partial \psi}{\partial r}\right) dr\right)\right] \tag{21c}$$

M_{11} and M_{21} are the fluid flow rate and electric current per unit pressure gradient, respectively, whereas M_{12} and M_{22} are the flow rate and electric current divided by the magnitude of E_z. The expression for M_{12} and M_{21} in Eq.(21b) is obtained from by-part integrating either the second term on the right hand side of Eq.(15) or that of Eq.(19). The fact that $M_{12} = M_{21}$ is an example of the Onsager reciprocal relation. The three electrokinetic phenomena discussed here can be understood directly from Eqs.(21a)-(21c) as discussed below.

Electroosmosis is a term referring to a fluid flow resulting from an applied electric field. Analogous to an osmotic flow where a fluid flow is caused by a solute concentration difference, an electroosmotic flow is caused by a voltage difference. When an electric field is applied along a charged channel in absence of an imposed pressure gradient (dP/dz = 0), the electric current is generated from the motion of the counterions in the electrical double layer ($I = M_{22}E_z$). A fluid flow rate ($Q = M_{21}E_z$) is established throughout the liquid as shown schematically in Fig. 3.

Streaming current, on the other hand, refers to an electric current caused by an imposed pressure difference where the electric potential at both channel ends is “forced” to be equal by using electrodes as shown in Fig. 4. At zero potential difference ($E_z = 0$) but non-zero pressure difference, a Poiseuille flow with $Q = -M_{11}(dP/dz)$ is created. The fluid flow carries the counter-ions, and as a result, the electric current often called the streaming current, $I = -M_{21}(dP/dz)$, is established and can be measured. The last of the three phenomena, streaming potential, occurs because, in an open circuit in absence of electrodes, there is no electric current. According to Eq.(20), if there is an imposed pressure gradient ($dP/dz \neq 0$), there must be a voltage difference,

resulting in a non-zero E_z;

$$E_z = \frac{M_{21}(dP/dz)}{M_{22}}. \tag{22}$$

The potential difference across the channel caused by the pressure difference is often called the streaming potential. The resulted fluid flow is a combination of an electro-osmotic flow and a Poiseuille flow, as shown schematically in Fig. 5.

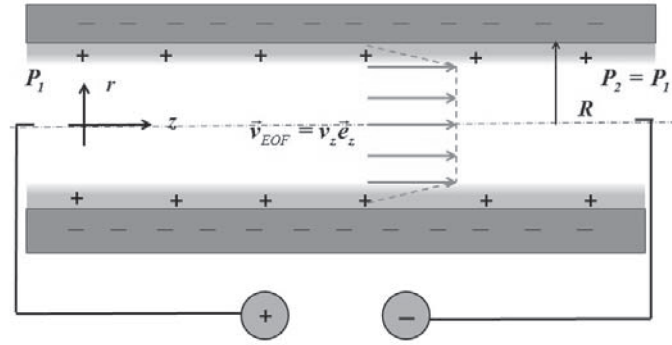

Figure 3 Schematic drawing of an electroosmotic flow in a negatively-charged microchannel. The channel cross-section is circular with radius R. The pressure at both ends of the channel are equal; $P_1 = P_2$. An electric field in the axial direction created by potential difference causes the motion of the positively charged counter-ions, resulting in the fluid velocity of an electroosmotic flow ($\vec{v}_{EOF}$). Outside the electrical double layer, $\vec{v}_{EOF}$ is uniform.

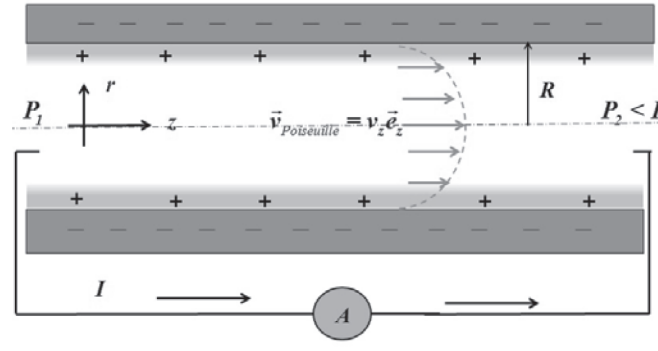

Figure 4 Schematic drawing of a streaming current in a negatively-charged channel. Electric potential at both channel ends are equal, whereas $P_1 > P_2$. The imposed pressure difference creates a Poiseuille flow that carries counter-ions and generates an electric current, I, often referred to as streaming current, in absence of voltage difference.

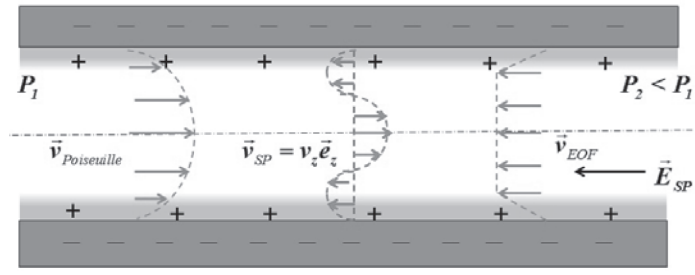

Figure 5 Schematic drawing of streaming potential ($\vec{E}_{SP}$) created in a negatively-charged channel. Because there is no electrode, the system is an open circuit and the total electric current, *I*, must be zero. An imposed pressure difference created $\vec{E}_{SP}$, and the resulted fluid velocity, $\vec{v}_{SP}$, is a superposition of a velocity of a Poiseuille flow and that of an electroosmotic flow.

It is worth noting that streaming potential is often considered a bit peculiar, especially from points of view of physicists who are familiar with Ohm's Law, because *I* is zero despite the non-zero potential difference. Likewise, streaming current is a non-zero electric current that can be generated even though the potential at both channel ends are equal.

Analytical solution for flows in weakly-charged channels

To illustrate the different profiles of fluid velocity during the three electrokinetic phenomena, a weakly-charged channel, where the Debye-Huckel approximation can be applied, is considered. The ionic concentration inside the channel with circular cross-section, assumed to retain its equilibrium distribution, can be approximated as follows.

$$C_i = C_i^0 \exp\left(\frac{-z_i e\varphi}{kT}\right) \approx C_i^0\left(1-\frac{z_i e\varphi}{kT}\right) \tag{23}$$

where $\varphi = \psi\left(r,z\right)-\psi\left(0,z\right)$ and C_i^0 is the concentration of ion *i* at the channel centerline (*r* = 0). Substituting Eq.(23) into Eq.(13), one obtains a governing equation for an electric potential in a dimensionless form as shown below [8].

$$\frac{1}{\tilde{r}}\frac{d}{d\tilde{r}}\left(\tilde{r}\frac{d\tilde{\varphi}}{d\tilde{r}}\right) = -\Gamma + \tilde{\varphi} \tag{24}$$

where $\tilde{\varphi} = \dfrac{\varphi}{kT/e}$. $\tilde{r} = \dfrac{r}{\lambda_0}$. $\Gamma = \dfrac{\sum_i z_i C_i^0}{\sum_i z_i^2 C_i^0}$. The length scale of the system is the Debye length

redefined based on the ionic concentration at the centerline of the channel as shown below.

$$\lambda_0 = \left(\frac{\varepsilon kT}{e^2 \sum_i z_i^2 C_i^0} \right)^{1/2} . \tag{25}$$

It is worth noting that $C_i^0 \neq 0$. A solution to Eq.(24) can be calculated analytically and can be written as

$$\tilde{\varphi} = \Gamma - \Gamma I_0 \left(\tilde{r} \right) \tag{26}$$

where $I_0 \left(\tilde{r} \right)$ is the modified Bessel function of the first kind of order zero. Eq.(26) is obtained under a condition that $\tilde{\varphi}\left(\tilde{r} = 0 \right) = 0$. The remaining unknown constant, Γ, must be evaluated from the surface charge density, q_e, as follows [7].

$$q_e = \varepsilon \left. \frac{\partial \varphi}{\partial r} \right|_{r=R} = \frac{\varepsilon kT}{\lambda_o e} \left. \frac{\partial \tilde{\varphi}}{\partial \tilde{r}} \right|_{\tilde{r}=R/\lambda_0} \tag{27}$$

Substituting the expression of the derivative of the dimensionless electric potential obtained from Eq.(26) into Eq.(27) yields

$$\Gamma = \frac{-\lambda_0 e q_e}{\varepsilon kT I_1 \left(R/\lambda_0 \right)} . \tag{28}$$

Substituting Γ back into Eq.(26), one obtains the dimensionless electric potential which leads to the fluid velocity (Eq.(14)) becoming

$$v_z = \frac{-\lambda_0 q_e E_z}{\eta} \frac{\left[I_0 (R/\lambda_0) - I_0 \left(r/\lambda_0 \right) \right]}{I_1 \left(R/\lambda_0 \right)} - \frac{dP}{dz} \frac{\left(R^2 - r^2 \right)}{4\mu} \tag{29}$$

During electroosmosis, dP/dz = 0. From Eq. (29), the fluid velocity in the axial direction, v_z^{EOF} is simply

$$v_z^{EOF} = \frac{-\lambda_0 q_e E_z}{\eta} \frac{\left[I_0 (R/\lambda_0) - I_0 \left(r/\lambda_0 \right) \right]}{I_1 \left(R/\lambda_0 \right)} \tag{30}$$

If $q_e > 0$, the counter-ions are anions. The direction of the electroosmotic flow is opposite to that of the imposed electric field. On the other hand, if $q_e < 0$, the counter-ions are cations and the fluid flows in the direction similar to that of the axial electric field as shown in Fig. 3. For very small values of λ_0 (compared to R), the fluid velocity outside the thin double layer becomes uniform. As $\lambda_0 \rightarrow 0$, the flow profile becomes similar to that of the plug flow (a flow with uniform velocity throughout the cross-section).

During the occurrence of a streaming current, $E_z = 0$ (because of the similar potential at both channel ends due to imposed electrodes) but $dP/dz \neq 0$. The fluid flow inside the charged channel is a parabolic Poiseuille flow that carries the counter-ions and generates a streaming current as shown in Fig.(4)

$$v_z^{Poiseuille} = -\frac{dP}{dz}\frac{\left(R^2 - r^2\right)}{4\eta} \tag{31}$$

As for the streaming potential, the fluid velocity in the axial direction (v_z^{SP}) can be found using an expression in Eq.(29) with E_z obtained as a function of dP/dz from Eq.(22) as shown below. If $q_e < 0$, the direction of E_z will be similar to that of the pressure gradient, whereas if $q_e > 0$, the directions of E_z and the imposed pressure gradient will be opposite. The fluid flow results from a superposition of an electroosmotic flow and a Poiseuille flow as shown earlier in Fig.(5).

$$v_z^{SP} = \frac{-dP}{dz}\left[\frac{\lambda_0 q_e M_{21}}{\eta M_{22}}\frac{\left[I_0(R/\lambda_0) - I_0\left(r/\lambda_0\right)\right]}{I_1\left(R/\lambda_0\right)} + \frac{\left(R^2 - r^2\right)}{4\eta}\right] \tag{32}$$

Applications of electroosmosis, streaming potential and streaming current

Electrokinetic phenomena mentioned above are employed for various applications in microsystems and microfluidic devices: the most notable being applications of electroosmosis. If a soluble substance is injected into a flow inside a channel, at first, a sharp peak of solute concentration is created. After a while, a phenomenon referred to as Taylor dispersion is observed where the peak broadens as a result of the transverse variation of the velocity in the field combined with the solute diffusion in all direction [7] as shown below in Fig. (6). Electroosmotic plug flow (which occurs if the Debye length is small compared to the dimension of the channel) permits transport of sample without sample broadening due to Taylor dispersion [4]. In addition, an integration of microelectrodes and power supply into the channel design allows generation and control of the electric field and an electroosmotic flow. Electrokinetic pumping, replacing purely mechanically driven parts that are often bulky, enables the devices to be portable [10, 11].

Furthermore, an electroosmotic flow can also be employed to facilitate effective mixing in microfluidic devices [12, 13]. Due to the fact that viscous dissipation dominates the momentum transfer in low Reynolds flows and turbulence is normally absent, streamlines do not intersect, and the flow is often unidirectional. Even in curved or twisted channels, the transverse component of the flow is very small compared to the axial component [14]. Several techniques involving electroosmosis were utilized in order to increase the mixing rate. An example is a

method called “electrokinetic focusing” where the sample (containing solutes) is introduced through the middle inlet of a T or a Y junction, and the solvent streams are introduced through the side inlets [15]. The sample stream width is reduced, and so is the mixing time. An insertion of this rapid mixer into microfluidic platforms makes studies of fast reaction kinetics such as microsecond kinetic studies of protein folding possible [16]. In addition, the heterogeneities of the surface charges on the channel walls have also been exploited to create localized recirculation regions within the flow in order to improve species mixing in the microchannel [17] as shown below in Fig. (7).

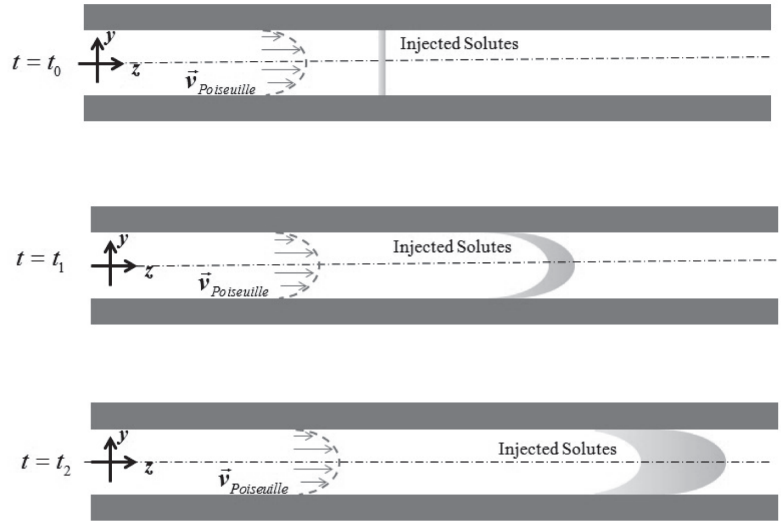

Figure 6 Schematic drawing of Taylor dispersion occurred in a microchannel containing a soluble substance injected into a Poiseuille flow. The size and direction of the arrows represent the magnitude and direction of fluid velocity, whereas shaded areas denote regions with injected solute concentration. At $t = t_0$, the soluble substance is injected into the flow, and the solute concentration exhibits a sharp uniform profile across the channel. Due to transverse variation of fluid velocity, solutes located at different transverse location are moving at different speeds. At later time ($t = t_1$), the solute concentration profile can be seen as non-uniform across the channel. In addition, because of solute diffusion in all directions, the solute concentration will gradually broaden axially. This becomes apparent at $t = t_2$. Electroosmotic plug flows observed at very low Debye length (compared to the channel sizes) with the fluid velocity being uniform at all transverse locations outside the electrical double layer are often employed to prevent Taylor dispersion in microchannels.

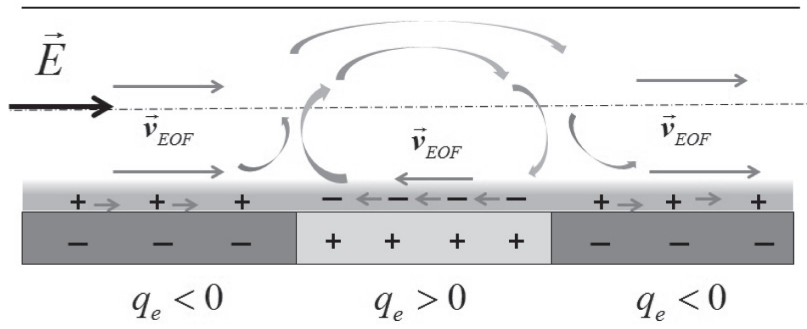

Figure 7 An example of how an electroosmotic flow contained in a channel with heterogeneous surface charge densities can be employed to improve specie mixing. A section of a very long channel where there is a heterogeneity in surface charge density is presented in the above schematic drawing. The direction of the flow and the electric field are indicated by the arrows. The base of the long channel is negatively charged everywhere except in a narrow section where its base is patterned with a band of positive surface charges. The motions in the opposite directions of cations and anions in the electrical double layer create an electroosmotic flow with a localized recirculation region. Figure is not drawn to scale.

Comparing to electroosmosis, the other two electrokinetic phenomena, streaming current and streaming potential, are less widely employed. Streaming potential measurement is used either to characterize the channel surface charges from the measured fluid flow rate, or to determine the flow rate if the channel surface charge density (or surface potential) is known [4, 18]. Likewise, a measurement of streaming current in channels is a sensitive method to characterize the channel surface potential.

Conclusion

Fluid mechanics of three electrokinetic phenomena with relevant microfluidic applications has been reviewed. Electroosmotic flow is a fluid flow driven by the potential difference, whereas, streaming current is an electric current generated by pressure difference inside the channel in absence of a voltage difference. Streaming potential, on the other hand, refers to a potential difference in an open-circuit microchannel generated by a pressure gradient. Applications of electroosmosis include prevention of sample broadening due to Taylor dispersion, fluid pumping and effective mixing, whereas applications of streaming current and streaming potential are mainly determination of channel surface charge density, surface potential and fluid flow rate.

References

1. Stone, H. A., and Kim, S. 2001. Microfluidics: Basic Issues, Applications and Challenges. *American Institute of Chemical Engineers Journal.* 47: 1250-1254.
2. Craighead, H. 2006. Future Lab-on-a-Chip Technologies for Interrogating Individual Molecules. *Nature.* 442: 387-393.
3. Whitesides, G. M. 2006. The Origins and the Future of Microfluidics. *Nature.* 442: 368-373.
4. Stone, H. A., Stroock, A.D., and Ajdari, A. 2004. Engineering Flows in Small Devices: Microfluidics Toward a Lab-on-a-Chip. *Annual Review of Fluid Mechanics.* 36: 381-411.
5. Saville, D.A. 1997. Electrokinetics Effects with Small Particles. *Annual Review Fluid Mechanics* 9: 321-337.
6. Russel, W.B., Saville, D. A., and Schowalter, W. R. 1999. Colloidal Dispersions. 3rd Edition. Cambridge. Cambridge University Press. p. 88-126.
7. Deen, W. M. 1998. Analysis of Transport Phenomena. 1st Edition. Oxford. Oxford University Press. p. 454-463.
8. Taylor, G. I. 1967. Low-Reynolds-Number Flows. Available from URL:http://techtv.mit.edu/collections/ifluids/videos/32604-low-reynolds-number-flow. 31 December 2016.
9. Newman, J. S. 1991. Electrochemical Systems. 2nd Edition. New Jersey. Prentice Hall. p. 215-225.
10. Chang, H. C. 2006. Electro-kinetics: A Viable Micro-fluidic Platform for Miniature Diagnostic Kits. *The Canandian Journal of Chemical Engineering.* 84: 146-160.
11. Luo, Y., Qin, J. H., and Lin, B. C. 2009. Methods for Pumping Fluids on Biomedical Lab-on-a-Chip. *Frontiers in Bioscience.* 14: 3913-3924.
12. Chang, CC., and Yang, RJ. 2007. Electrokinetic Mixing in Microfluidic Systems. *Microfluidics and Nanofluidics.* 3: 507-525.
13. Qian, S., and Bau, H. H. 2002. A Chaotic Electroosmotic Stirrer. *Analytical Chemistry.* 74: 3616-3625.
14. Chen, JK., and Luo, WJ., and Yang RJ. 2006. Electroosmotic Flow Driven by DC and AC Electric Fields in Curved Microchannels. *Japanese Journal Applied Physics.* 45: 7983-7990.
15. Yang, RJ., Chang CC., Huang SB., and Lee GB. 2005. A New Focusing Model and Switching Approach for Electrokinetic Flow Inside Microchannels. *Journal of Micromechanics and Microengineering* 15: 2141-2148.

16. Hertzog, D. E., Michaelet, X., Jager M., Kong, X., Santiago, J. G., Weiss, S., and Bakajin, O. 2004. Femtomole Mixers for Microsecond Kinetic Studies of Protein Folding. *Analytical Chemistry.* 76: 7169-7178.
17. Erickson, D., and Li, D. 2002. Influence of Surface Heterogeneity on Electrokinetically Driven Microfluidic Mixing. *Langmuir.* 18: 1883-1892.
18. Li, D. 2004. Electrokinetics in Microfluidics Volume 2. 1st Edition. New York. Elsevier Academic Press. p. 30-44.

ได้รับบทความวันที่ 6 ตุลาคม 2559
ยอมรับตีพิมพ์วันที่ 9 มกราคม 2560